Insulin Kinetics in Type-1 Diabetes: Continuous and Bolus Delivery of Rapid Acting Insulin

Malgorzata E. Wilinska, Ludovic J. Chassin, Helga C. Schaller, Lukas Schaupp, Thomas R. Pieber, and Roman Hovorka*, *Member, IEEE*

***Abstract*—We investigated insulin lispro kinetics with bolus and continuous subcutaneous insulin infusion (CSII) modes of insulin delivery. Seven subjects with type-1 diabetes treated by CSII with insulin lispro have been studied during prandial and postprandial conditions over 12 hours. Eleven alternative models of insulin kinetics have been proposed implementing a number of putative characteristics. We assessed 1) the effect of insulin delivery mode, i.e., bolus or basal, on the insulin absorption rate, the effects of 2) insulin association state and3) insulin dose on the rate of insulin absorption, 4) the remote insulin effect on its volume of distribution, 5) the effect of insulin dose on insulin disappearance, 6) the presence of insulin degradation at the injection site, and finally 7) the existence of two pathways, fast and slow, of insulin absorption. An iterative two-stage parameter estimation technique was used. Models were validated through assessing physiological feasibility of parameter estimates, posterior identifiability, and distribution of residuals. Based on the principle of parsimony, best model to fit our data combined the slow and fast absorption channels and included local insulin degradation. The model estimated that 67(53–82)% [mean (interquartile range)] of delivered insulin passed through the slow absorption channel [absorption rate 0.011(0.004–0.029) min^{-1}] with the remaining 33% passed through the fast channel [absorption rate 0.021(0.011–0.040) min^{-1}]. Local degradation rate was described as a saturable process with Michaelis–Menten characteristics [$V_{MAX} = 1.93(0.62 - 6.03)$ mU min^{-1}, $K_M = 62.6(62.6 - 62.6)$ mU]. Models representing the dependence of insulin absorption rate on insulin disappearance and the remote insulin effect on its volume of distribution could not be validated suggesting that these effects are not present or cannot be detected during physiological conditions.**

***Index Terms*—Biological systems modeling, identification, insulin kinetics, parameter estimation, type-1 diabetes.**

I. Introduction

INSULIN therapy in people with type-1 diabetes aims to mimic the pattern of endogenous insulin secretion present in healthy subjects. This pattern can be achieved to some extent by continuous subcutaneous insulin infusion (CSII) with an insulin pump administering individually titrated basal insulin infusion and prandial insulin boluses. Despite considerable progress, currently available insulin preparations do not fully deliver the desired insulin profile, partly due to the delay in the appearance of insulin in the plasma following subcutaneous injection. Absorption of regular insulin from the subcutaneous depot is impeded by the formation of hexameric macromolecules. The DNA-recombinant technique has contributed to the synthesis of rapid acting human insulin analogues such as lispro, with a reduced formation of higher order hexamers and with binding to the receptors and biological activity preserved [1]. As this type of insulin is absorbed faster from the subcutaneous tissue, its ability to mimic the physiological pattern of insulin secretion is improved [2]. For that reason lispro and, for that matter, other fast acting insulin analogues have become the insulin of choice for the CSII therapy [1]. The availability of rapid acting analogue also opened new opportunities for the development of a wearable artificial pancreas (WAP), a research goal of the last decade. A better understanding of the insulin absorption process could lead to further improvements in glycaemic control and, in relation to the WAP, could help to increase predictive powers of the WAP algorithm. However, the pharmacokinetics of subcutaneous insulin is yet to be fully described. The absorption from the subcutaneous tissue is influenced by many factors including the associated state of insulin, i.e., hexameric, dimeric, or monomeric [3], concentration and injected volume [4], injection site and depth [5], [6], and blood flow [7]. Several models of subcutaneous insulin kinetics have been proposed [8]–[13] dealing with different types of commercially available insulin preparations. As insulin analogues are a recent innovation, only two of those models [11], [13] consider monomeric rapid acting insulin such as lispro. Shimoda *et al.* [13] used a simple three-compartmental linear model, equivalent to Model 1 presented in this study, to derive their closed-loop insulin infusion algorithm. Trajanoski and colleagues [12] used a different approach. They modified and approximated a noncompartmental model with distributed parameters by Mosekilde *et al.* [14]. In order to reduce the complexity of the model, the authors made a number of assumptions. One of such simplifications, for instance, was an assumption that the sc injected insulin forms a spherical homogenous depot. Since the model by Trajanoski *et al.* was theoretically unidentifiable [15], the formal identification techniques could not be used. Therefore, the parameter values for this model were not estimated but were chosen from published *in vivo* and *in vitro* studies.

The aim of this study was to investigate the kinetics of insulin lispro during a standard insulin pump treatment with bolus and

Manuscript received July 3, 2003; revised May 9, 2004. This work was supported in part by the 5th European Commission (EC) Framework Programme under Grant IST-1999-14027 (ADICOL) and in part by the 6th EC Framework Programme under Grant IST-2002-506965 (CLINICIP). *Asterisk indicates corresponding author.*

M. E. Wilinska and L. J. Chassin are with the Department of Paediatrics, University of Cambridge, Cambridge, CB2 2QQ, U.K. (e-mail: mew37@medschl.cam.ac.uk; ljc45@medschl.cam.ac.uk).

H. C. Schaller is with the Department of Biophysics, Institute of Biomedical Engineering, University of Technology, A-8036 Graz, Austria (e-mail: schaller@microperfusion.at).

L. Schaupp and T. R. Pieber are with the Department of Internal Medicine, Diabetes and Metabolism, Medical University of Graz, A-8036 Graz, Austria (e-mail: schaupp@microperfusion.at; pieber@healthgate.at).

*R. Hovorka is with the Department of Paediatrics, University of Cambridge, Cambridge, CB2 2QQ, UK (e-mail: r.hovorka@uk.avecho.com).

Digital Object Identifier 10.1109/TBME.2004.839639

TABLE I
PROPOSED COMPARTMENT MODELS OF INSULIN LISPRO KINETICS

Model	Compartment Structure	* Equations	Comments	Parameters
1		$dQ_1/dt=u-k_{a1}Q_1$ [Eq. 1] $dQ_2/dt=k_{a1}Q_1 - k_{a1}Q_2$ [Eq. 2] $dQ_3/dt=k_{a1}Q_2 - k_eQ_3$ [Eq. 3]	Basic linear model	V, k_{a1}, k_e
2	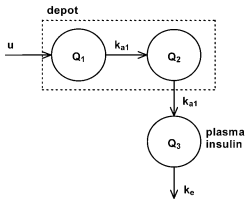	$dQ_1/dt=u-(-a_1Q_1+k_{a1})Q_1$ $dQ_2/dt=(-a_1Q_1+k_{a1})Q_1 - (-a_1Q_2+k_{a1})Q_2$ $dQ_3/dt=(-a_1Q_2+k_{a1})Q_2 - k_eQ_3$	Saturable insulin absorption rate - simplified MM form	V, a_1, k_{a1}, k_e
3		$dQ_1/dt=u-V_{MAX,a}Q_1/(k_{M,a}+Q_1)$ $dQ_2/dt= V_{MAX,a}Q_1/(k_{M,a}+Q_1)$ $- V_{MAX,a}Q_2/(k_{M,a}+Q_2)$ $dQ_3/dt= V_{MAX,a}Q_2/(k_{M,a}+Q_2) - k_eQ_3$	Saturable insulin absorption rate – MM relation	V, $V_{MAX,a}$, $k_{M,a}$, k_e
4		Equations 1, 2 and 3 $k_{a1}=V_{MAX,e}/(k_{M,e}+Q_3)$	Saturable insulin disappearance	V, $V_{MAX,e}$, $k_{M,e}$, k_{a1}
5	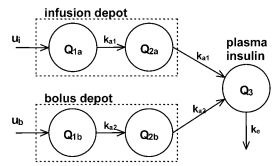	$dQ_{1a}/dt=u_i-k_{a1}Q_{1a}$ $dQ_{1b}/dt=u_b-k_{a2}Q_{1b}$ $dQ_{2a}/dt=k_{a1}Q_{1a} - k_{a1}Q_{2a}$ $dQ_{2b}/dt=k_{a2}Q_{1b} - k_{a2}Q_{2b}$ $dQ_3/dt=k_{a1}Q_{2a} + k_{a2}Q_{2b} - k_eQ_3$	Delivery mode dependent insulin absorption rate	V, k_{a1}, k_{a2}, k_e
6	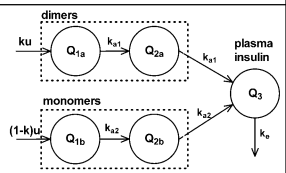	$dQ_{1a}/dt=ku-k_{a1}Q_{1a}$ $dQ_{1b}/dt=(1-k)u-k_{a2}Q_{1b}$ $dQ_{2a}/dt=k_{a1}Q_{1a} - k_{a1}Q_{2a}$ $dQ_{2b}/dt=k_{a2}Q_{1b} - k_{a2}Q_{2b}$ $dQ_3/dt=k_{a1}Q_{2a} + k_{a2}Q_{2b} - k_eQ_3$	Dimers-monomers equilibrium	V, k_{a1}, k_{a2}, k_e, k
7	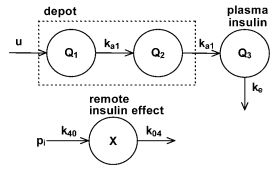	$dQ_1/dt=u-k_{a1}Q_1$ $dQ_2/dt=k_{a1}Q_1 - k_{a1}Q_2$ $dQ_3/dt=k_{a1}Q_2 - k_eQ_3$ $dX/dt=k_{40}pi - k_{04}X$ and $k_{40}=1$ $V=V_0(1+V_{MAX}X/(k_M+X))$	Remote insulin effect on its volume of distribution	V, k_{a1}, k_e, k_{04} V_{MAX}, k_M
8	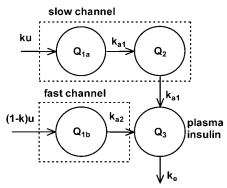	$dQ_{1a}/dt=ku-k_{a1}Q_{1a}$ $dQ_{1b}/dt=(1-k)u-k_{a2}Q_{1b}$ $dQ_2/dt=k_{a1}Q_{1a} - k_{a1}Q_2$ $dQ_3/dt=k_{a1}Q_2 + k_{a2}Q_{1b} - k_eQ_3$	Slow and fast insulin absorption channels	V, k_{a1}, k_{a2}, k_e, k
9		as above and $u = u_i + Bu_b$	Relative bio-availability of bolus to continuous infusion	k_{a1}, k_{a2}, k_e, k, B

continuous infusion modes of insulin delivery as it may be used in a WAP.

II. METHODS

A. Subjects and Experimental Protocol

Seven subjects with type-1 diabetes (4/3 F/M, age 31.7 ± 14.1 years, $\mathrm{HbA_{1c}}$ 8.5 ± 1%, BMI 26.2 ± 4.9 $\mathrm{kg/m^2}$, daily basal insulin requirements 23.6 ± 6.4 U/day; mean ± SD) treated by CSII participated in the study. All subjects had nondetectable C-peptide levels. The participants provided written informed consent, and the study was approved by the local ethics committee. Six subjects (Subject 1–6) were studied after an overnight fast (start of the study at 8:00) and one subject (Subject 7) was studied at postprandial conditions overnight (start of the study at 19:00). The subjects arrived at the University Hospital, University of Graz, Austria, one hour prior to the start of the study and remained in supine position for the 12 hours of the experiment.

On arrival at the hospital, an intravenous cannula was inserted into a forearm vein to facilitate arterialised venous blood sampling using a thermoregulated (55 °C) box. A replacement cannula was inserted into the subcutaneous abdominal tissue for the variable administration of rapid acting insulin analogue (Humalog, Eli Lilly) (lispro) by an insulin pump (D-Tron, Disetronic Medical Systems, Burgdorf, Switzerland).

At the start of the study, the subjects ingested a standard meal [40-gram (g) carbohydrates (CHO)] with a co-administration of

TABLE I
(*Continued.*)
PROPOSED COMPARTMENT MODELS OF INSULIN LISPRO KINETICS

Model	Compartment Structure	* Equations	Comments	Parameters
10	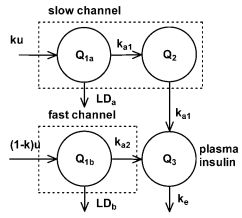	$dQ_{1a}/dt=ku-k_{a1}Q_{1a}-LD_a$ $dQ_{1b}/dt=(1-k)u-k_{a2}Q_{1b}-LD_b$ $dQ_2/dt=k_{a1}Q_{1a}-k_{a1}Q_2$ $dQ_3/dt=k_{a1}Q_2+k_{a2}Q_{1b}-k_eQ_3$ $LD_a=V_{MAX,LD}Q_{1a}/(k_{M,LD}+Q_{1a})$ $LD_b=V_{MAX,\,LD}Q_{1b}/(k_{M,LD}+Q_{1b})$	Local degradation of insulin at the injection site	V, k_{a1}, k_{a2}, k_e, k, $V_{MAX,LD}$, $k_{M,LD}$
11	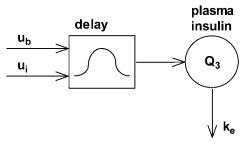	$dQ_3/dt=-k_eQ_3+A(t)$ $A(t)=u_b t^{s-1}sT_{50,b}^{s}/\left(T_{50,b}^{s}+t^{s}\right)^2+\int_0^t u_i(\tau)\frac{(t-\tau)^{s_i-1}s_iT_{50,i}^{s_i}}{\left(T_{50,i}^{s_i}+(t-\tau)^{s_i}\right)^2}d\tau$ $T_{50,b}=au_b+b$ $T_{50,i}=b_i$	Empirically derived insulin absorption function	V, k_e, s, s_i, a, b, b_i

In all models, $i=Q_3/V$

an individually determined prandial insulin bolus. Only water was allowed for the rest of the study. In case of a low plasma glucose (PG) concentration (<3.3 mmol/l) a bolus of 10–20 g of intravenous glucose (20% Dextrose solution, Fresenius Kabi, Graz, Austria) was administered.

Arterialised venous blood samples were drawn every 15 min for the determination of PG and every 30 min for the determination of plasma insulin. Plasma insulin was measured using the Iso-Insulin ELISA (Mercodia AB, Uppsala, Sweden) assay with an intra-assay CV <6%. PG was measured every 15 min on a bedside analyzer and the insulin infusion rate was changed every 15 min based on the advice of the MPC algorithm [16], with an aim to maintain normoglycaemia at postprandial conditions.

B. Modeling Insulin Kinetics

Eleven alternative compartment models were postulated to represent the insulin kinetics following the administration of a bolus and continuous infusion of insulin lispro (Table I).

The models differed in the description of subcutaneous insulin absorption and its elimination from plasma. We assessed 1) the effect of insulin delivery mode, i.e., bolus or basal, on the insulin absorption rate, the effects of 2) insulin association state and 3) insulin dose on its rate of absorption, 4) the remote insulin effect on its volume of distribution, 5) the effect of insulin dose on insulin disappearance, 6) the presence of insulin degradation at the injection site, and finally 7) the existence of two pathways, fast and slow, of insulin absorption.

Plasma insulin was represented by a single compartment in all models. Insulin in the subcutaneous tissue was represented by two compartments to describe the delay in insulin absorption, or by one compartment to represent a faster absorption channel.

Model 1 was a basic three compartment linear model, in which both the insulin absorption rate and the insulin disappearance rate were assumed unaffected by other factors.

Model 2 assumed a linear relationship between insulin absorption rate and the amount of insulin infused.

Model 3 assumed saturable insulin absorption rate with an increasing insulin dose. The saturable process was implemented as the Michaelis–Menten relationship between the insulin absorption rate and the insulin dose. The two delivery modes, continuous infusion and bolus, were not discriminated by this model.

Model 4 assumed a saturable, dose dependent insulin disappearance rate implemented in a Michaelis–Menten form. The absorption rate was assumed linear and independent of the insulin delivery mode.

Model 5 differentiated among continuous insulin infusion and the bolus administration and assumed that the insulin absorption rate is dependent on the delivery mode with the aim to assess whether, as frequently discussed in literature, insulin administered in the form of a bolus is absorbed more slowly than insulin given as a continuous infusion.

In Model 6, it was assumed that certain amount of the injected monomeric insulin associates to form dimmers and that a state of equilibrium is reached between the two association states. The insulin absorption rate was assumed to be different for monomers and dimers. No nonlinearities were included in this model.

Model 7 examined the remote insulin effect on its volume of distribution. The relationship between plasma insulin and the volume of distribution was assumed to take a Michaelis–Menten form.

Model 8 considered two different pathways of insulin absorption, one consisting of two compartments, as in the previously described models, and the other with one compartment turning it into a faster channel for insulin absorption. The proportion of insulin channeled through these two pathways was considered to be the same for the two delivery modes, continuous infusion and the bolus. This and following models were formulated to over-

come underestimation of the postprandial plasma insulin peak encountered by the previous models.

Model 9 introduced bioavailability of the insulin bolus relative to that of the continuous infusion while maintaining the two pathways of insulin absorption implemented in Model 7. This relative bioavailability is sometimes referred to in literature as an effectiveness factor and could be explained by different levels of local insulin degradation of bolus and infusion delivery modes.

Model 10 considered local degradation of insulin at the injection side, also maintaining the two pathways of insulin absorption (as in Model 8). The degradation process was assumed to be saturable and was implemented as a Michaelis–Menten relation.

Finally, Model 11 is based on that published by Berger *et al.* [11] and describes insulin absorption using a noncompartment formulation derived from published studies [17], [18].

Formal definitions of models are shown in Table I. The explanation of symbols is as follows: i is plasma insulin (mU L^{-1}; Q_1 and Q_2 represent insulin mass (mU) in the accessible and nonaccessible subcutaneous compartments, respectively; Q_{1a} and Q_{2a} represent mass of insulin administered as continuous infusion (Model 5) or mass of insulin associated into dimers (Model 6) (mU), and Q_{1b} and Q_{2b} represent mass of insulin given as a bolus (Model 5) or mass of insulin maintaining monomeric form (Model 6) (mU); Q_3 represents insulin mass (mU) in the plasma compartment; V represents the insulin distribution volume (L kg^{-1}); u represents the insulin input (mU min^{-1}), u_i and u_b (mU min^{-1}) represent the continuous insulin infusion and the bolus input, respectively; k_{a1}, k_{a2}, k_{04}, k_{40} and k_e are transfer rates (min^{-1}), a_1 is the slope of saturable insulin absorption (min^{-1} mU L^{-1}); $V_{MAX,a}$ and $V_{MAX,e}$ are the maximal values of insulin flux (mU min^{-1}) describing the Michaelis–Menten dynamics of insulin absorption and insulin disappearance respectively; $k_{M,a}$ and $k_{M,e}$ are values of insulin mass (mU) at which insulin flux is equal to half of its maximal value when describing the Michaelis–Menten dynamics of insulin absorption and disappearance, respectively; X is the remote insulin effect in (mU L^{-1}), k_M is the value of insulin concentration at which the distribution volume attains half of its maximal value (mU L^{-1}), and V_{MAX} (unitless) is the maximum proportional increase in the volume of distribution; $V_{MAX,LD}$ is the saturation level (mU min^{-1}) describing Michaelis–Menten dynamics of insulin degradation for continuous infusion and bolus; $k_{M,LD}$ is the value of insulin mass (mU) at which insulin degradation is equal to half of its maximal value for continuous infusion and bolus; B (unitless) is the relative bioavailability of the insulin bolus to the continuous infusion; LD_a and LD_b represent local degradation at the injection site (mU min^{-1}) for continuous infusion and bolus, respectively; k (unitless) is the proportion of the total input flux passing through the slower, two compartment channel (Models 8–10) or a proportion of insulin associated into dimeric form in the sc pool (Model 6); s and s_i (unitless) characterize the absorption rate of bolus and continuous infusion respectively, $T_{50,b}$ is the time to reach 50% absorption of the injected insulin bolus (min) with a (min U^{-1}) and b (min) used as parameters, and $T_{50,i}(= b_i)$ is the time interval (min) to reach 50% absorption of the continuous infusion. All models are *a priori* identifiable [15].

C. Parameter Estimation

To reflect the skewed distribution of model parameters, prior to the estimation process, all parameters except k and B were log-transformed. This also assured nonnegativity of those parameters. The parameters were then estimated using an iterative two-stage (ITS) population kinetic analysis [19], [20]. In each iteration, model parameters were estimated employing a nonlinear, weighted, least-squares algorithm with an empirical Bayesian term.

The weight was defined as the reciprocal of the square of the measurement error, which was assumed to have a zero mean and a coefficient of variation of 6%. This measurement error was assumed to be constant across both subjects and measurements.

The accuracy of parameter estimates was obtained from the Fisher information matrix [15]. The SAAM II Population Kinetics v 1.2 (SAAM Institute, Seattle, WA) was employed to carry out the calculations.

D. Iterative Two-Stage Analysis

Model parameters were estimated using ITS population kinetic analysis.

ITS is a parametric iterative population analysis method based on the concepts of population prior knowledge and maximum *a posteriori* (MAP) probability empirical Bayes estimator [20]. There are three steps of ITS: Step 1) initialization, Step 2) expectation, and Step 3) minimization. In the initialization step, the population mean for each parameter is calculated as the sample mean of all the individual parameter estimates. Population variance is also calculated as the corresponding sample variance. In Step 2, the expectation step, parameter estimation for each individual subject $\mathbf{j}$ is performed again, this time minimizing the following extended MAP Bayesian objective function with respect to $\mathbf{p_j}$ [21]

$$MAP(\boldsymbol{p_j}) = \sum_{i=1}^{N_j} \frac{\left[G_{i,j}^{D} - G^{M}(p_j, t_{i,j})\right]^2}{\sigma_{i,j}^2} + \sum_{i=1}^{N_p} \frac{\left[\mu_i(k) - p_{j,i}\right]^2}{\hat{\sigma}_{i,i}^2(k)} \tag{1}$$

where the distance of the current parameter estimate from the population mean is also penalized; we denote with $p_{j,i}$ the ith element of the parameter vector $\mathbf{p_j}$ for subject j, $\mu_i(k)$ is the value of the population mean at the kth iteration, N_j is the number of data points available for the jth subject, $t_{i,j}$ and $G_{i,j}^{D}$ are the ith time point and data point, respectively, for the jth subject, $\sigma_{i,j}^2$ is the variance of the measurement error of the ith data point, $G^{M}(p_j, t_i)$ is the model prediction for a given p_j, and $\sigma_{i,i}^2(k)$ is the ith diagonal element of the population covariance matrix at the kth iteration. The estimate obtained by minimizing this objective function is called post hoc, or empirical Bayes, estimate. An updated population mean of the parameter vector and the covariance are calculated. In the final Step 3, the check for convergence of the population mean, the population variance, and the individual parameter estimates is carried out. This is done by determining whether or not the current and the previous estimate differ by $<1\%$. If so, the algorithm is stopped, if not, it returns to Step 2. Hence, Step 2 and 3 are performed iteratively until the convergence is reached.

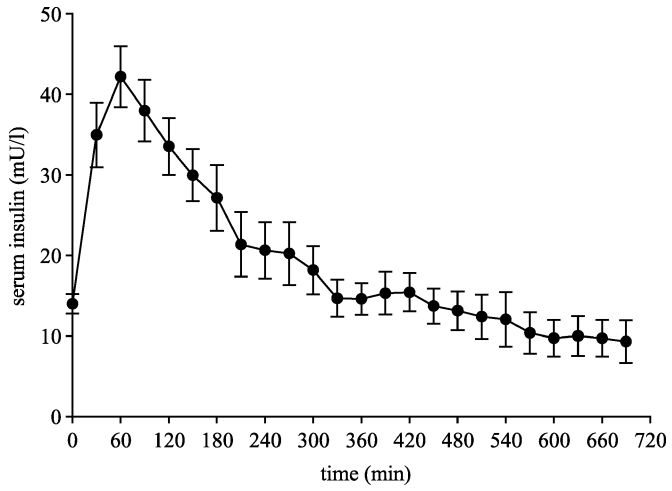

Fig. 1. Plasma insulin concentration. Values are mean ± SE.

E. Model Identification and Validation

Parameter estimates were checked for physiological feasibility. To validate the models, two additional criteria were adopted. These were posterior identifiability and the distribution of residuals [15]. Posterior identifiability of each model was assessed on the basis of the accuracy of parameter estimates. A given parameter was considered nonidentifiable if the coefficient of variation of the parameter estimate was $\gg 150\%$. The Runs test evaluated the randomness of the residuals.

F. Model Selection

The best model, i.e., the model, which best represented our experimental data with the minimum number of parameters, was selected using the principle of parsimony. The two most commonly used tests that implement this principle are the Akaike criterion (AIC) [22] and the Bayesian information criterion (BIC), also known as Schwarz [23]. The two tests are defined as follows:

$$\mathrm{AIC} = N\ln(\mathrm{WRSS}) + 2P \tag{2}$$

$$\mathrm{BIC} = N\ln(\mathrm{WRSS}) + P\ln N \tag{3}$$

where N is the number of data points, WRSS is the weighted residual sum of squares, and P is the number of parameters.

As the number of data points in this study was small (N range from 18 to 28), the two tests would give similar results [see (2) and (3)]. The author chose to implement AIC in this study, although BIC was also calculated by SAAM II software package.

III. Results

A. Experimental Data

Mean plasma insulin concentration is shown in Fig. 1. The continuous insulin infusion rate, which varied during the experiments, was 0.86 ± 0.27 U/h (mean ± SD), and the bolus administered prior to the meal was 5.95 ± 2.37 U.

B. Model Identification and Validation

Model identification and validation results are summarized in Table II. Models 4 and 7 proved nonidentifiable with precision

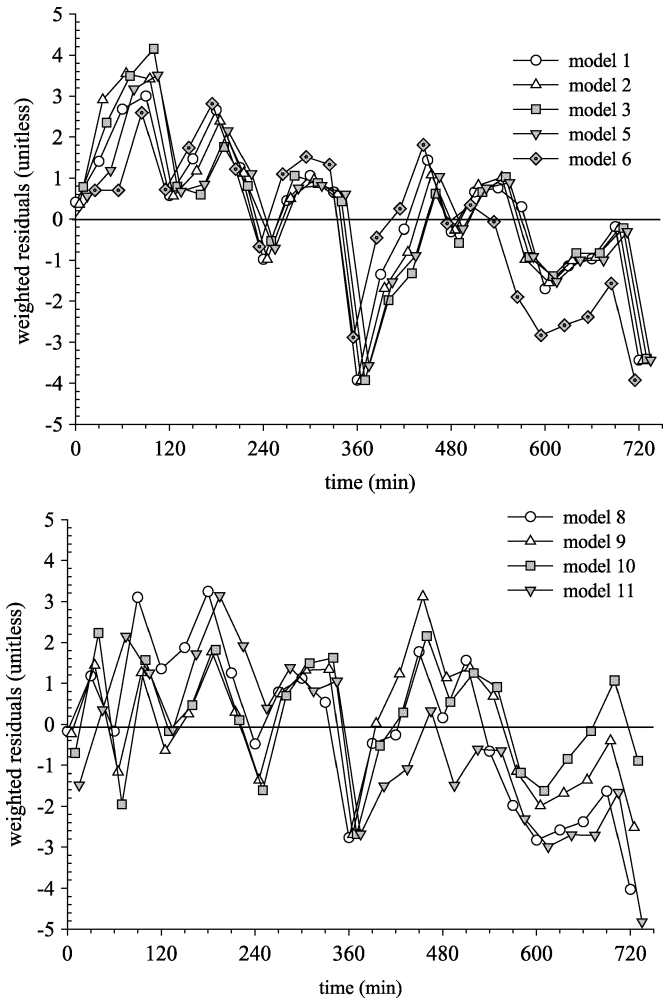

Fig. 2. Mean weighted residuals for Model 1, 2, 3, 5 and 6 (top panel) and Model 8, 9, 10 and 11 (bottom panel) (n = 7).

of parameter estimates for $\mathrm{K_M}$, $\mathrm{V_{MAX}}$, $\mathrm{K_{M,e}}$, and $\mathrm{V_{MAX,e}}$, expressed as CV considerably exceeding 150% in most of the individual cases. The remaining eight models demonstrated physiological feasibility of parameter estimates and posterior identifiability, see Table II. Weighted residuals associated with these models are plotted in Fig. 2. The results of the Runs test applied to the weighted residuals, i.e., the percentage of cases, which passed this test, are shown in Table II. Weighted residuals of models 2, 9, 10, and 11 passed the Runs test in 100% of cases (see Table II).

C. Model Selection

The values of AIC for *a posteriori* identifiable models are shown in Table II. On the basis of this criterion, Model 10 was selected as best representing the experimental data. This model is also characterized by 100% of cases passing the Runs test and the tightest range of the weighted residuals (see Fig. 2). Although parameter estimates for $\mathrm{k_e}$ and V were outside the physiological limits defined from the validated studies, their product, the metabolic clearance rate (MCR), maintained physiological feasibility. The parameter estimates for this model and for all the other *a posteriori* identifiable models are shown in Tables III(a), III(b), and III(c). An example model fit generated by Model 10 is shown in Fig. 3.

TABLE II
MODEL IDENTIFICATION, VALIDATION AND SELECTION. SUMMARY RESULTS

Model	Physiological feasibility Yes/No	Precision of parameter estimates Good/Acceptable/ Unacceptable**	Runs Test %*	Akaike score Mean ± SD
1	Yes	Acceptable	86	8.06 ± 6.08
2	Yes	Acceptable	100	7.62 ± 5.85
3	Yes	Good	57	7.78 ± 5.86
4	Yes	Unacceptable	N/A	N/A
5	Yes	Good	71	7.43 ± 6.10
6	Yes	Good	86	5.39 ± 3.02
7	Yes	Unacceptable	N/A	N/A
8	Yes	Good	86	6.11 ± 3.41
9	Yes	Good	100	4.32 ± 2.37
10	Yes	Good	100	4.13 ± 2.12
11	Yes	Good	100	6.17 ± 3.59

*Percentage of random cases
** Good (CV<100%), Acceptable (CV<150%), Unacceptable (CV>150%)

IV. DISCUSSION

Mathematical modeling is a common approach to quantify subcutaneous insulin absorption. A number of models have been proposed [8]–[14] dealing with different insulin types. Two of those models [12], [13] consider monomeric rapid acting insulin, such as lispro.

Our 11 models are partly or, in case of Model 11, entirely based on existing models of insulin kinetics after sc insulin injection. For instance, Model 1 has an identical structure to that by Puckett *et al.* [10] with an omitted effectiveness factor to represent local insulin degradation. In our study, the effect of local insulin degradation at the injection site was accounted for in Models 9 and 10. In Model 9, instead of Puckett's effectiveness factor, we use relative bioavailability B to account for different levels of insulin degradation for the bolus and continuous infusion modes of delivery. Although this model proved identifiable, the model fit was not as good as that of the best Model 10.

Model 11 is the only noncompartmental model based on empirical equation describing subcutaneous insulin absorption derived by Berger *et al.* [24]. This model was also identifiable with borderline physiological values of parameter estimates but did not provide the best fit to the experimental data.

Except Models 1 and 6, all other models are nonlinear. Nonlinearity with Michaelis–Menten characteristics was imposed on insulin absorption (Model 3), insulin disappearance (Model 4), the remote insulin effect on the volume of distribution (Model 7), and finally on the local insulin degradation (Model 10).

Several authors [4], [9], [12], [14], [25] observed that the insulin absorption rate varies inversely with the concentration of the injected insulin. Trajanoski *et al.* [12], in their theoretical study, examined this phenomenon in the monomeric insulin and found its absorption rate to be constant regardless of the concentration and volume. This finding was supported indirectly by Kang *et al.* [3] who studied the influence of molecular aggregation on rates of subcutaneous absorption. Our Models 2 and 3 addressed this issue of concentration dependent absorption rate by assuming nonlinear dynamics and saturability of subcutaneous insulin absorption. Model 2 uses a simplified,

TABLE III(a)
PARAMETER ESTIMATES FOR IDENTIFIABLE MODELS. VALUES ARE POPULATION MEANS (INTER-QUARTILE RANGE OF INDIVIDUAL VALUES) ($N = 7$)

Model	k_{a1} ($10^{-2}\times$ min^{-1})	k_{a2} ($10^{-2}\times$ min^{-1})	k_e ($10^{-2}\times$ min^{-1})	k (unitless)	V (10^{-2} x L kg^{-1})	MCR (10^{-3} x L kg^{-1} min^{-1})
1	1.66 (1.04 – 2.66)	--	30.22 (6.79 – 134.55)	--	5.38 (1.16 – 25.07)	16.3 (13.1 – 20.1)
2	1.83* (1.05 – 3.19)	--	36.17 (8.57 – 152.70)	--	4.49 (1.03 – 19.68)	16.2 (13.1 – 20.1)
3	--	--	41.50 (15.45 - 111.49)	--	3.90 (1.46 – 10.39)	16.2 (13.1 – 19.9)
5	1.89 (0.97 – 3.66)	1.58 (1.03 – 2.43)	28.58 (7.56 - 108.03)	--	5.62 (1.42 – 22.26)	16.1 (12.9 – 20.0)
6	1.81 (0.69 – 4.74)	4.00 (2.07 – 7.72)	2.02 (1.75 – 2.32)	0.41 (0.24 – 0.57)	75.93 (64.58 – 82.46)	15.3 (11.7 – 20.1)
7	1.89 (1.00 – 3.57)	2.57 (1.34 – 4.95)	1.91 (1.54 – 2.37)	0.71 (0.60 – 0.82)	84.00**	16.0 (12.9 – 19.9)
8	2.47 (1.69 – 3.61)	0.79 (0.18 – 3.34)	1.98 (1.32 – 2.97)	0.57 (0.44 – 0.70)	86.13 (59.11 – 125.50)	17.1 (12.4 – 23.5)
9	1.12 (0.44 – 2.85)	2.10 (1.12 – 3.96)	1.89 (1.34 – 2.68)	0.67 (0.53 – 0.82)	56.45 (38.79 – 82.16)	10.7 (6.3 – 18.1)
10	--	--	3.68 (1.33 – 10.20)	--	42.01 (16.73 – 105.51)	15.5 (12.5 – 19.1)

*Estimate of k_{a1} at zero insulin concentration
**Individual values converged to an identical estimate

whereas Model 3 a full form of the Michaelis–Menten relation. Both models proved only borderline identifiable with precision of some parameter estimates exceeding 100%. In particular, $V_{MAX,a}$ and $K_{M,a}$, the Michaelis–Menten parameters in Model 3, achieved borderline precision for some but not all subjects. The highest CV for $V_{MAX,a}$ was 123% and for $K_{M,a}$ 124% indicating higher degree of uncertainty related to these parameter estimates. In the case of Model 2, borderline CVs were recorded for V, the volume of distribution, and k_e, insulin disappearance rate.

As already stated, Kang *et al.* [3] studied the influence of molecular aggregation on rates of sc insulin absorption. The authors found differing absorption rates of hexamers, dimers, and monomers. The fastest absorption rates were demonstrated with monomeric, while the slowest with hexameric insulin. In Model 6, we assume that the injected monomeric insulin partially associates to form dimers in the subcutaneous depot. Assuming an equilibrium state between dimers and monomers, Model 6 considered two separated pools for the two association states of the injected insulin and two different absorption rates (see Table I, Model 6). Model 6 was *a posteriori* identifiable with a good precision of parameter estimates. It was estimated that approximately 41% of the injected insulin was in a dimeric form characterized by a slower absorption rate [see Table III(a)]. The difference between the two absorption rates, however, was not statistically significant ($p = 0.11$; paired t-test).

The evidence of a saturable insulin removal in the supraphysiological range of the insulin concentration has been demonstrated in several studies [26]–[28]. In the physiological range of the insulin concentration, however, the existing evidence points to a linear process [29]. A nonlinear kinetics of the insulin removal rate is adopted by Model 4. This model proved *a posteriori* nonidentifiable with a CV of three of the parameter estimates (V, $V_{MAX,e}$, and $K_{M,e}$) exceeding 150%. A low precision of the Michaelis–Menten parameters suggests that saturable levels of the plasma insulin concentration were not achieved during our experiment and that the insulin disappearance is most probably linear over the physiological range.

Mosekilde *et al.* [14] observed an inverse relationship between the insulin absorption rate and the injected volume. This implies that insulin kinetics depends on the insulin delivery mode, i.e., it is different for bolus (a large volume) and the continuous subcutaneous infusion (a sequence of small volumes). Other authors [8] did not find such dependence in their studies. In Model 5, we examined this finding for insulin lispro. The bolus and continuous infusion inputs were routed via separate absorption channels. The insulin absorption rate constants for bolus and infusion were estimated and were not different ($p = 0.34$, paired t-test). We acknowledge that the continuous mode of insulin delivery used in our study differed from the standard approach, where the insulin infusion rate is changed less frequently. However, changing the insulin infusion rate

TABLE III(b)
PARAMETER ESTIMATES FOR MODELS 2, 3, 8, AND 9. VALUES ARE POPULATION MEANS (INTER-QUARTILE RANGE OF INDIVIDUAL VALUES) ($N = 7$)

Model	$V_{MAX,a}$ (10^3 x mU min^{-1})	$k_{M,a}$ (10^3 x mU)	$V_{MAX,LD}$ (mU min^{-1})	$k_{M,LD}$ (mU)	B (unitless)	a_1 (10^{-8} x min^{-1} $mmol^{-1}$ L)
2	--	--	--	--	--	14.8 (2.1 – 105.4)
3	1.14 (0.36 - 3.67)	66.0 (15.1 – 288.8)	--	--	--	--
8	--	--	--	--	1.55 (1.14 – 1.95)	--
9	--	--	1.93 (0.62 – 6.03)	62.6 (62.6 – 62.6)	--	--

*Individual values converged to an identical estimate

TABLE III(c)
PARAMETER ESTIMATES OF A, B, B_I, S, AND S_I VALUES ARE POPULATION MEANS (INTER-QUARTILE RANGE OF INDIVIDUAL VALUES) ($N = 7$)

a ($min\ U^{-1}$)	b (min)	b_i (min)	s (unitless)	s_i (unitless)
2.44 (1.66 – 3.59)	53.45 (30.97 – 92.27)	79.19 (36.47 – 171.97)	2.01 (1.74 – 2.32)	2.86 (1.91 – 4.26)

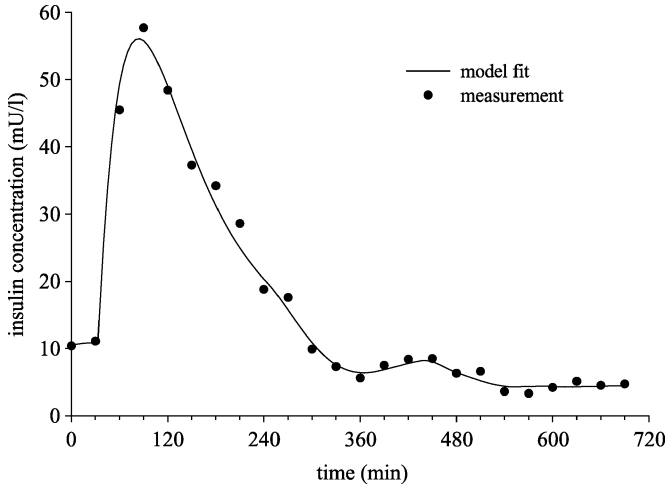

Fig. 3. Example fit for Model 10.

every 15 min provided a richer dynamic behavior and was more representative of the insulin delivery to be used in an artificial pancreas.

It has been suggested that insulin may have a remote effect on its volume of distribution [30]. This remote effect of insulin was represented in Model 7. Unfortunately, Model 7 was not *a posteriori* identifiable with a CV for V_{MAX} and K_M reaching values as high as 300%.

Although several of the already discussed models were *a posteriori* identifiable, the post meal peak of plasma insulin was consistently underestimated. We therefore introduced two, slow and fast, insulin absorption channels differing in the number of compartments. A marked improvement in the model fit was observed in Models 8, 9, and 10, which include the two absorption channels. The best model fit was observed in Models 9 and 10, which further implement local insulin degradation. Although the volume of distribution and the insulin elimination rate from plasma were not physiologically feasible in Models 9 and 10, the MCR of insulin attained physiological feasibility [see Table III(a)]. For this reason, the two models were retained and Model 10, with a slightly lower Akaike value, was selected as best representing our data (see Fig. 3 for an example model fit). The value of insulin MCR obtained by Model 10 is almost identical with that obtained by Kraegen *et al.* [9] with an independent intravenous experiment (10.8 mL/min for regular insulin) and Shimoda *et al.* [13] (10.6 mL/min for monomeric insulin).

The presence of the local insulin degradation is a controversial issue. Some studies confirm its significance [31], [32], others discount it as relatively small [4], [9], [33]. In Model 10, we modeled the local degradation as a saturable Michaelis–Menten process. The mean precision of $V_{MAX,LD}$ estimate was very good (47 ± 58%; mean ± SD) with the exception of one subject with a value of 150%. Parameter estimates for $K_{M,LD}$ almost converged to the population mean in all subjects. The mean precision of each of the parameter estimates in this model was less than 50%. Our best model indicates that the effect of insulin degradation, however small [$V_{MAX,LD} = 1.93(0.62 - 6.03)$ mU min^{-1},

$K_{M,LD} = 62.6(62.6 - 62.6)\mathrm{mU}]$, is not, as suggested by Binder *et al.* [4], insignificant in the physiological range of insulin concentrations.

As far as the two absorption channels are concerned, Model 10 estimated that 67(53–82)% [mean(interquartile range)] of insulin passes through the slow absorption channel [absorption rate 0.011(0.004–0.029) min^{-1}] with the remaining 33% passing through the fast channel [absorption rate 0.021(0.011–0.040) min^{-1}]. The idea of two absorption channels does not have an immediate physiological interpretation.

Marked intersubject variability of the insulin absorption rate from the subcutaneous tissue has been observed by many authors [12], [14], [34]. The insulin absorption is thought to be dependent on the injection site [5], [6], the injection depth [35], lipodystrophy [36], low body weight [36] and many other factors such as exercise, smoking, temperature etc. The intersubject variability can be seen very clearly across all individual parameter estimates of Model 10.

V. Conclusion

Eleven alternative models of insulin lispro kinetics have been evaluated and validated with experimental data collected in subjects with type-1 diabetes. The selection process based on the AIC identified Model 10 as best representing our data. The model suggests the presence of fast and slow absorption channels and the presence of local insulin degradation.

References

v

[1] J. L. Jameson, "Update: insulin lispro: a new, rapidly acting analogue," in *Harrison's Principles of Internal Medicine*, E. Braunwald, A. S. Fauci, K. J. Isselbacher, D. L. Kasper, S. L. Hauser, D. L. Longo, and J. L. Jameson, Eds. New York: McGraw-Hill, 1999.

[2] S. Kang, F. M. Creagh, J. R. Peters, J. Brange, A. Volund, and D. R. Owens, "Comparison of subcutaneous soluble human insulin and insulin analogues (AspB9, GluB27; AspB10; AspB28) on meal-related plasma glucose excursions in type I diabetic subjects," *Diabetes Care*, vol. 14, no. 7, pp. 571–577, July 1991.

[3] S. Kang, J. Brange, A. Burch, A. Volund, and D. R. Owens, "Subcutaneous insulin absorption explained by insulin's physicochemical properties. Evidence from absorption studies of soluble human insulin and insulin analogues in humans," *Diabetes Care*, vol. 14, no. 11, pp. 942–948, Nov. 1991.

[4] C. Binder, "Absorption of injected insulin. A clinical-pharmacological study," *Acta Pharmacol. Toxicol.*, vol. 2, pp. 1–84, 1969.

[5] V. A. Koivisto and P. Felig, "Alterations in insulin absorption and in blood glucose control associated with varying insulin injection sites in diabetic patients," *Ann. Intern. Med.*, vol. 92, no. 1, pp. 59–61, 1980.

[6] M. Berger, H. J. Cuppers, H. Hegner, V. Jorgens, and P. Berchtold, "Absorption kinetics and biologic effects of subcutaneously injected insulin preparations," *Diabetes Care*, vol. 5, pp. 77–91, 1982.

[7] G. Nucci and C. Cobelli, "Models of subcutaneous insulin kinetics. A critical review," *Comput. Meth. Programs Biomed.*, vol. 62, no. 3, pp. 249–257, July 2000.

[8] T. Kobayashi, S. Sawano, T. Itoh, K. Kosaka, H. Hirayama, and Y. Kasuya, "The pharmacokinetics of insulin after continuous subcutaneous infusion or bolus subcutaneous injection in diabetic patients," *Diabetes*, vol. 32, no. 4, pp. 331–336, Apr. 1983.

[9] E. W. Kraegen and D. J. Chisholm, "Insulin responses to varying profiles of subcutaneous insulin infusion: kinetic modeling studies," *Diabetologia*, vol. 26, pp. 208–213, 1984.

[10] W. R. Puckett and M. Lightfoot, "A model for multiple subcutaneous insulin injections developed from individual diabetic patient data," *Am. J. Physiol.*, vol. 269, pp. E1115–E1124, 1995.

[11] M. Berger and D. Rodbard, "Computer-simulation of plasma-insulin and glucose dynamics after subcutaneous insulin injection," *Diabetes Care*, vol. 12, pp. 725–736, 1989.

[12] Z. Trajanoski, P. Wach, P. Kotanko, A. Ott, and F. Skraba, "Pharmacokinetic model for the absorption of subcutaneously injected soluble insulin and monomeric insulin analogs," *Biomedizinische Technik*, vol. 38, pp. 224–231, 1993.

[13] S. Shimoda, K. Nishida, M. Sakakida, Y. Konno, K. Ichinose, M. Uehara, T. Nowak, and M. Shichiri, "Closed-loop subcutaneous insulin infusion algorithm with a short-acting insulin analog for long-term clinical application of a wearable artificial endocrine pancreas," *Front Med. Biol. Eng.*, vol. 8, no. 3, pp. 197–211, 1997.

[14] E. Mosekilde, K. S. Jensen, C. Binder, S. Pramming, and B. Thorsteinsson, "Modeling absorption kinetics of subcutaneous injected soluble insulin," *J Pharmacokinet. Biopharm.*, vol. 17, no. 1, pp. 67–87, Feb. 1989.

[15] E. R. Carson, C. Cobelli, and L. Finkelstein, *The Mathematical Modeling of Metabolic and Endocrine Systems*, 1st ed. New York: Wiley, 1983.

[16] R. Hovorka, V. Canonico, L. J. Chassin, U. Haueter, M. Massi-Benedetti, M. Orsini-Federici, T. R. Pieber, H. Schaller, L. Schaupp, T. Vering, and M. Wilinska, "Non-linear model predictive control of glucose concentration in subjects with type 1 diabetes," *Physiol. Meas.*, vol. 25, pp. 905–920, 2004.

[17] C. Binder, T. Lauritzen, O. Faber, and S. Pramming, "Insulin pharmacokinetics," *Diabetes*, vol. 7, pp. 188–199, 1984.

[18] D. R. Owens, *Clinical Pharmacological Studies in Normal Man*. Hingham, MA: MTP, 1986.

[19] J. L. Steimer, A. Mallet, J. L. Golmard, and J. F. Boisvieux, "Alternative approaches to estimation of population pharmacokinetic parameters: comparison with the nonlinear mixed-effect model," *Drug Metabol. Rev.*, vol. 15, pp. 265–292, 1984.

[20] R. Hovorka and P. Vicini, "Parameter estimation," in *Modeling Methodology for Physiology and Medicine*, E. R. Carson and C. Cobelli, Eds. San Diego, CA: Academic, 2001, pp. 107–151.

[21] P. Vicini and C. Cobelli, "The iterative two-stage population approach to IVGTT minimal modeling: improved precision with reduced sampling. Intravenous glucose tolerance test," *Am. J. Physiol.*, vol. 280, no. 1, pp. E179–E186, Jan. 2001.

[22] H. Akaike, "A new look at the statistical model identification," *IEEE Trans. Autom. Control*, vol. AC-19, pp. 716–723, 1974.

[23] G. Schwarz, "Estimating the dimension of a model," *Ann. Statist.*, vol. 5, no. 2, pp. 461–464, 1978.

[24] M. P. Berger and D. Rodbard, "A pharmacodynamic approach to optimizing insulin therapy," *Comput. Meth. Programs Biomed.*, vol. 34, pp. 241–253, 1991.

[25] A. Murat and G. Slama, "Influence of concentration on the kinetics of sc-infused insulin. Comparison between square-wave SC infusion and bolus SC injection," *Metabolism*, vol. 34, pp. 120–123, 1985.

[26] P. H. Sonksen, C. V. Tompkins, M. C. Srivastava, and J. D. N. Nabarro, "A comparative study on the metabolism of human insulin and porcine proinsulin in man," *Clin. Sci. Molec. Med.*, vol. 45, pp. 633–654, 1973.

[27] K. G. Tranberg, "Hepatic uptake of insulin in man," *Am. J. of Physiol.*, vol. 237, pp. E509–E518, 1979.

[28] E. Ferrannini, J. Wahren, O. K. Faber, P. Felig, C. Binder, and R. A. DeFronzo, "Splanchnic and renal metabolism of insulin in human subjects: a dose-response study," *Am. J. Physiol.*, vol. 244, pp. E517–E527, 1983.

[29] D. P. Frost, M. C. Srivastava, R. H. Jones, J. D. N. Nabarro, and P. H. Sonksen, "The kinetics of insulin metabolism in diabetes mellitus," *Postgrad. Med. J.*, vol. 49, pp. 949–954, 1973.

[30] E. H. Serne, R. G. IJzerman, R. O. B. Gans, R. Nijveldt, G. de Vries, R. Evertz, A. J. M. Donker, and C. D. A. Stehouwer, "Direct evidence for insulin-induced capillary recruitment in skin of healthy subjects during physiological hyperinsulinemia," *Diabetes*, vol. 51, no. 5, pp. 1515–1522, 2002.

[31] M. Berger, P. A. Halban, L. Girardier, J. Seydoux, R. E. Offord, and R. E. Renold, "Absorption kinetics of subcutaneously injected insulin. Evidence for degradation at the injection site," *Diabetologia*, vol. 17, pp. 97–99, 1979.

[32] A. E. Kitabchi, F. B. Stentz, C. Cole, and W. C. Duckworth, "Accelerated insulin degradation: an alternate mechanism for insulin resistance," *Diabetes Care*, vol. 2, pp. 414–417, 1979.

[33] S. Kang, J. Brange, A. Burch, A. Volund, and D. R. Owens, "Absorption kinetics and action profiles of subcutaneously administered insulin analogues (AspB9GluB27, AspB10, AspB28) in healthy subjects," *Diabetes Care*, vol. 14, no. 11, pp. 1057–1065, Nov. 1991.

[34] T. Lauritzen, O. K. Faber, and C. Binder, "Variation in ^{125}I-insulin absorption and blood glucose concentration," *Diabetologia*, vol. 17, pp. 291–295, 1979.

[35] P. Hildebrandt, P. Sejrsen, S. L. Nielsen, K. Birch, and L. Sestoft, "Diffusion and polymerization determines the insulin absorption from subcutaneous tissue in diabetic patients," *Scand. J. Clin. Lab. Invest.*, vol. 45, pp. 685–690, 1985.

[36] K. Kolendorf, J. Bojsen, and T. Deckert, "Clinical factors influencing the absorption of ^{125}I-NPH insulin in diabetic patients," *Hormone Metabol. Res.*, vol. 15, pp. 274–278, 1983.

Malgorzata E. Wilinska received the M.Sc. degree in electronic engineering majoring in medical and nuclear electronics from the Technical University of Warsaw, Warsaw, Poland, in 1988. After moving to the U.K., she gained clinical experience working in the National Health Service as a qualified nurse. She received the M.Sc. degree in medical informatics from Kings College, London, U.K., in 1998. In 2004, she received the Ph.D. degree in measurement and instrumentation in medicine from City University, London, U.K.

From 2001–2004, she was a Research Assistant at City University, London, and worked on a successful EU-funded ADICOL project, which developed novel solutions to control insulin delivery in type-1 diabetes. In February 2004, she moved to the University of Cambridge, Cambridge, U.K., where she is involved in another European project CLINICIP continuing her work in the area of glucose control. Her main interests are in the field of modeling and simulation in physiology with a main focus on diabetes.

Ludovic J. Chassin received M.Sc. degree in information engineering in 1997 from City University, London, U.K., and Research Associate training in Sup-Sante, Paris.

He has been appointed for different research contracts involving modeling and simulation in physiology. From 2000–2004, he has been working on the EU-funded FP5 IST project ADICOL aiming at the development of a closed-loop insulin delivery system at City University where he also registered as a Ph.D. staff candidate. He is currently continuing his work in modeling and simulation of glucose metabolism as a consultant for Roche Diagnostics, Burgdorf, Switzerland, and at the University of Cambridge, Cambridge, U.K., where he has an honorary Ph.D. student position.

Helga C. Schaller was born in Brunico (Bolzano), Italy, in 1971. She received the M.Sc. degree in electrical engineering from the Graz University of Technology, Graz, Austria, in 2000.

Since 2000, she has been with the Institute of Biomedical Engineering, Graz University of Technology and the Medical University Graz. Her main research activities are in the field of subcutaneous glucose monitoring and the extracorporeal artificial beta cell.

Lukas Schaupp was born in Fürstenfeld,Austria, in 1965. He received the Diploma and Ph.D. degrees in biomedical engineering from Graz University of Technology, Graz, Austria, in 1992 and 1998, respectively.

In 1995, he attended the Postgraduate Internship Program at Whiting School of Engineering at Johns Hopkins University, Baltimore, MD, (Applied Physics Laboratory). From 1998–2001, he was a Research Fellow at the Karl Franzens University Graz. Since 2001, he is with the Joanneum Research, Institute of Medical Technologies and Health Management, Austria. His main interests are sampling techniques and biosensors for metabolites in interstitial fluid with particular interest in diabetes research.

Thomas R. Pieber received the M.D. degree from the Karl-Franzens-University School of Medicine in Graz, Austria, in 1987. He had training in intensive care medicine, endocrinology, and metabolism at the Karl-Franzens-University, Graz,Austria, at the Heinrich-Heine-University Düsseldorf, Germany, and at the University of Texas, Dallas.

Since 1993, he has been Senior Attending Staff with the Department of Internal Medicine at the Karl-Franzens-University Graz, Divison Diabetes and Metabolism. In 1997, he became Associate Professor at the Karl-Franzens-University Graz and in 2000 he was nominated as Vice Medical Director of the University hospital of Graz. Since 2001, he has been Director of the Institute of Medical Technologies and Health Management, Joanneum Research, Graz, which covers research for the development and evaluation of medical systems, investigation of mechanisms of action, data and health management and bioanalytics for medical research.

Dr. Pieber's current and previous positions include serving as Chairman and organizer of the Postgraduate Course in Clinical Diabetology on behalf of the European Association for the Study of Diabetes (EASD), Co-founder and member of the International Institute of Quality Assurance in Diabetology Austria (FQSD-Ö), and President of the Austrian Diabetes Association (ÖDG).

Roman Hovorka (M'90) received the B.Sc., M.Sc., and Ph.D. degrees in mathematical informatics and theoretical cybernetics from Charles University, Prague, Czech Republic, in 1984 and 1989, respectively

From 1984-1989, he was Research Fellow at Third Medical Faculty, Charles University, Prague, In 1989, he joined the City University, London, U.K., supported by two-year Fellowship from Wellcome Trust. Following a three-year joint postdoctoral position with Glaxo Wellcome, he founded and headed Metabolic Modeling Group based in the Centre for Measurement and Information in Medicine (MIM), City University. From 1998 to 2003 he was Reader at the MIM Centre while holding an honorary adjunct position at St. Thomas' Hospital, London, U.K. In 2004, he moved to the University of Cambridge, Cambridge, U.K., where he established Diabetes Modeling Group in the Department of Paediatrics. He was Scientific Coordinator of the EU Biomed 2 project *DiabStyle* dealing with decision support systems in diabetes. He contributed to the successful outcome of the EU-funded FP5 IST project *ADICOL*, which developed novel solutions to control insulin delivery in type-1 diabetes. His research activities comprise modeling, simulation, control, and decision support in medicine in general and in diabetes in particular. He has published over 60 papers in internationally refereed journals. He is currently on the Editorial Board of *Nutrition & Metabolism*.

Since 1998, Dr. Hovorka has been a Chartered Engineer. He is a member of the Institution of Electrical Engineers, Diabetes U.K., the European Association for Study of Diabetes, American Diabetes Association, and the American Physiological Society.